Direct photon pair measurement at DØ

L. HAN
Department of Modern Physics, University of Science and Technology of China (USTC), Hefei, Anhui 230026, P.R.China

We present a measurement of direct photon pair production cross sections using $4.2fb^{-1}$ of data collected with the D0 detector at the Fermilab Tevatron $p\bar{p}$ Collider. We measure single differential cross sections as a function of the diphoton mass, the transverse momentum of the diphoton system, the azimuthal angle between the photons and the polar scattering angle of the photons, and double differential cross sections considering the last three kinematic variables in three diphoton mass bins. The results are compared with different perturbative QCD predictions and event generators.

The direct photon pair (DPP) production with large invariant mass at hadron colliders is of special interesting. It constitutes large irreducible background for Higgs decaying into diphoton mode, and new heavy resonances and extra dimensions searches. Thus, precise measurements of the diphoton differential production cross sections for various kinematic variables and their theoretical understanding are extremely important for future Higgs and new phenomena searches. On the other hand, providing opportunity of verifying the validity of the predictions of perturbative quantum chromodynamics (pQCD) and soft-gluon resummation methods implemented in theoretical calculations, diphoton production itself is interesting. In this letter, we present a brief report on the precise measurements of DDP production at the D0 experiment in $p\bar{p}$ collisions at $\sqrt{s} = 1.96\ TeV$ at the Tevatron Collider. With large integrated luminosity, the double differential cross sections of this process are measured for the first time, detail can be found in [1].

The dominant $p\bar{p} \to \gamma\gamma + X$ production mode is via quark scattering $q\bar{q} \to \gamma\gamma$, then followed by gluon fusion as $gg \to \gamma\gamma$. Although the gluon fusion contribution is governed by quark-loop diagrams at leading order (LO) and suppressed by a factor of α_s^2 compared to the quark scattering processes, it would be significantly enhanced by gluon patron density in low invariant mass $M_{\gamma\gamma}$ region. For example, the expected fraction of gluon fusion to the total DPP rate can reach more than 10% when $M_{\gamma\gamma} < 100\ GeV$, predicted by by the PYTHIA [2] Monte Carlo (MC) event generator with the CTEQ6.1L [3] parton distribution function (PDF) set. In addition, direct photons may be produced from single or double parton-to-photon fragmentation processes of the partons produced in the hard scattering [4,5]. There are two next-to-leading order (NLO) theoretical predictions on DPP production in pQCD, namely RESBOS [4] and DIPHOX [5]. In DIPHOX, gluon fusion contribution is considered only at LO, but the explicit fragmentation effects are included up to NLO, while in RESBOS an approximate NLO fragmentation function is adopted. Also, only in RESBOS, the resummation of initial state gluon soft and collinear emissions is taken into account to all orders.

The DPP production cross sections are measured by using $4.2fb^{-1}$ data collected by D0

experiment from August 2006 to June 2009. The cross sections are measured differentially as a function of the diphoton invariant mass $M_{\gamma\gamma}$ and transverse momentum $p_T^{\gamma\gamma}$, the azimuthal angle between the photons $\Delta\phi_{\gamma\gamma}$, and the cosine of the polar scattering angle of the photon in the frame with no net transverse momentum of the diphoton system. These kinematic variables probe different aspects of the DPP production mechanism, for example, the shapes of the $p_T^{\gamma\gamma}$ and $\Delta\phi_{\gamma\gamma}$ distributions are mostly affected by initial state gluon radiation and fragmentation effects. The invariant mass $M_{\gamma\gamma}$ spectrum is particularly sensitive to potential contributions from new phenomena.

The D0 detector is discussed in detail elsewhere [6]. Events are selected by requiring two photon candidates with transverse momentum $p_T > 21(20)\ GeV$ for the leading(trailing) p_T photon and pseudorapidity $|\eta| < 0.9$. The photon p_T is computed with respected to the reconstructed primary vertex with the highest number of associated tracks in the event. The asymmetry p_T cuts for the two photon candidates are required to suppress the impact of kinematic region $p_T^{\gamma\gamma} \to 0(\Delta\phi_{\gamma\gamma} \to \pi)$, where the NLO pQCD calculation diverges. The photon candidates are selected by requiring to deposit most of its energy in the electromagnetic (EM) calorimeter layers, and the energy weighted EM shower shape be consistent with that expected for an electromagnetic shower. The EM cluster energy must be isolated in the calorimeter, $[E_{tot}(0.4) - E_{EM}(0.2)]/E_{EM}(0.2) < 0.1$, where $E_{tot}(R)$ and $E_{EM}(R)$ are the total energy and the energy in the EM section, respectively, within a cone of radius $R = \sqrt{(\Delta\eta)^2 + (\Delta\phi)^2} = 0.2$ around the photon direction. To minimize electrons misidentified as photons, the EM candidates are required to not be spatially matched to significant tracker activity. This track-match veto suppress background contributions from Drell-Yan events $Z/\gamma^* \to e^+e^-$, where both electrons are misidentified as photons. To further suppress a jet misidentified as a single photon resulting from fluctuations in the parton fragmentation into a well-isolated neutral meson (π^0 or η) decay into a final state with two or more photons, an artificial neural network discriminant O_{NN} is developed by exploiting differences in the tracker activity and energy deposits in the EM calorimeter and the central preshower detector between photons and jets. The O_{NN} is trained using single photon and jet PYTHIA MC samples and the performance is verified using a data event sample consisting of photons radiated from charged leptons in Z boson decays ($Z \to l^+l^-\gamma, l = e, \mu$). A loose $O_{NN} > 0.3$ cut is required, which offers nearly full efficiency for photons and rejects 40% of the jet faked photons. Finally, the two photon candidates are required to be spatially separated as $\Delta R > 0.4$ and satisfy invariant mass cut as $M_{\gamma\gamma} > p_T\gamma\gamma$. The mass requirement, together with photon isolation cut, significantly remove the component of fragmentation contribution in DPP events, therefore restricting the data-to-theory comparison to the region where the theoretical calculations should have smaller uncertainties.

After imposing all above requirements, the selected data sample includes Drell-Yan and QCD γ+jet and dijet instrumental background. The contribution from Drell-Yan events is estimated using the MC simulation with PYTHIA, normalized to the NNLO cross section. The charge misidentification rate determined from the MC simulation are corrected to those measured in the data. Backgrounds due to γ+jet and dijet events are estimated from data by using a 4×4 matrix background estimation method [7]. A tighter $O_{NN} > 0.6$ is employed to divide the data events into four orthogonal categories, depending on whether the leading/trailing p_T photon candidates pass (p) or fail (f) this requirement. The corresponding number of events, after subtracting the estimated Drell-Yan contribution, compose a 4-component vector $(N_{pp}, N_{pf}, N_{fp}, N_{ff})$. The difference in relative efficiencies of the $O_{NN} > 0.6$ between photons and jets allows estimation of the sample composition by solving a linear system of equations: $(N_{pp}, N_{pf}, N_{fp}, N_{ff})^T = \epsilon \times (N_{\gamma\gamma}, N_{\gamma j}, N_{j\gamma}, N_{jj})^T$, where $N_{\gamma\gamma}(N_{jj})$ is the number of DPP (dijet) events and $N_{\gamma j}(N_{j\gamma})$ is the number of γ+jet events with the leading(trailing) p_T photon candidate being a real photon. The 4×4 matrix ϵ contains the photon ϵ_γ and jet ϵ_j efficiencies, estimated using photon and jet MC samples and validated in data.

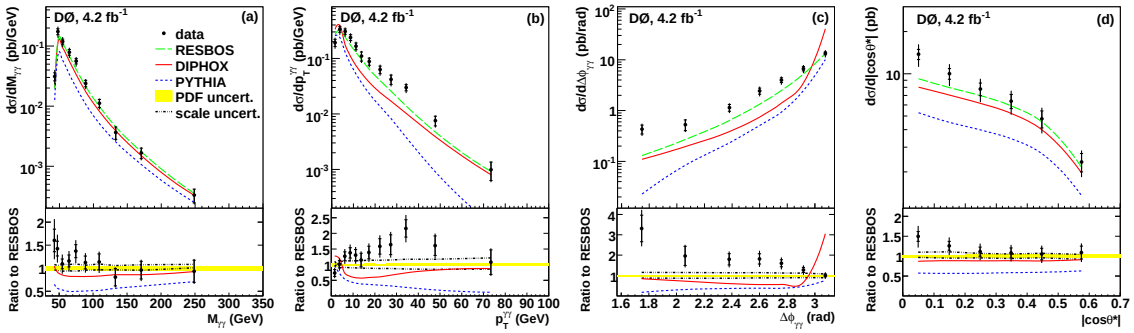

Figure 1: The measured differential diphoton production cross sections as functions of (a)$M_{\gamma\gamma}$, (b)$p_T^{\gamma\gamma}$, (c) $\Delta\phi_{\gamma\gamma}$ and (d) $|\cos\theta^*|$. The data are compared to the theoretical predictions from RESBOS, DIPHOX, and PYTHIA. The ratio of differential cross sections between data and RESBOS are displayed as black points with uncertainties in the bottom plots. The inner line for the uncertainties in data points shows the statistical uncertainty, while the outer line shows the total uncertainty. The solid (dashed) line shows the ratio of the predictions from DIPHOX (PYTHIA) to those from RESBOS. In the bottom plots, the scale uncertainties are shown by dash-dotted lines and the PDF uncertainties by shaded regions.

The estimated number of DPP events $N_{\gamma\gamma}$ in each kinematic bin is corrected for the DPP event selection efficiency and acceptance. The event efficiency is calculated using PYTHIA MC and processed through a GEANT-based simulation of the D0 detector. Differences between data and MC in the per-photon selection efficiencies are corrected for with suitable scale factors derived using control samples of electrons from Z boson and its radiative decays. The acceptance is calculated using DPP events generated with RESBOS. The differential cross sections $d\sigma/dM_{\gamma\gamma}$, $d\sigma/dp_T^{\gamma\gamma}$, $d\sigma/d\Delta\phi_{\gamma\gamma}$ and $d\sigma/d|\cos\theta^*|$ are obtained from the number of data events corrected for the background contribution, divided by the trigger, vertex and diphoton selection efficiencies, acceptance, integrated luminosity, and the bin width for each kinematic variable. The dominant systematic uncertainties include γ+jet and dijet background substraction resulting from the uncertainties on ϵ_γ and ϵ_j and typically varying within (11-15)%, the common uncertainties of photon selection criteria (4.3%) and luminosity (6.1%).The measured differential cross sections, compared to the theoretical predictions from RESBOS, DIPHOX and PYTHIA, are depicted in Fig. 1

The results obtained show that none of the theoretical predictions considered is able to describe the data well in all kinematic regions of the four variables. RESBOS shows the best agreement with data, although systematic discrepancies are observed at low $M_{\gamma\gamma}$, high $p_T^{\gamma\gamma}$ and low $\Delta\phi_{\gamma\gamma}$, the agreement is fair at intermediate $50 < M_{\gamma\gamma} < 80\ GeV$ and good at high $M_{\gamma\gamma} > 80\ GeV$. The large discrepancy between RESBOS and DIPHOX in some regions of the phase space is due to absence of all-order soft-gluon resummation and accounting $gg \to \gamma\gamma$ contribution only at LO in DIPHOX.

Further insight on the dependence of the $p_T^{\gamma\gamma}$, $\Delta\phi_{\gamma\gamma}$ and $|\cos\theta^*|$ kinematic distributions on the mass scale can be gained through the measurement of double differential cross sections. For instance, the differential cross sections as functions of $p_T^{\gamma\gamma}$ are measured in three $M_{\gamma\gamma}$ bins: $30-50\ GeV$, $50-80\ GeV$ and $80-350\ GeV$. The results are presented in Fig.2 , corresponding to each of the three $M_{\gamma\gamma}$ intervals. These results confirm that the discrepancies between data and RESBOS originate are largest in the lowest mass region $M_{\gamma\gamma} < 50\ GeV$, where the contribution from gluon fusion is expected to be largest, while are reduced in the intermediate region, and good description of all kinematic variables can be achieved for the $M_{\gamma\gamma} > 80\ GeV$ high mass region, the relevant region for the Higgs boson and new phenomena searches. It should be noticed that at the Tevatron, DPP production at high masses is strongly dominated by $q\bar{q}$ annihilation, in contrast with the LHC, where the contribution from gg and qg initiated

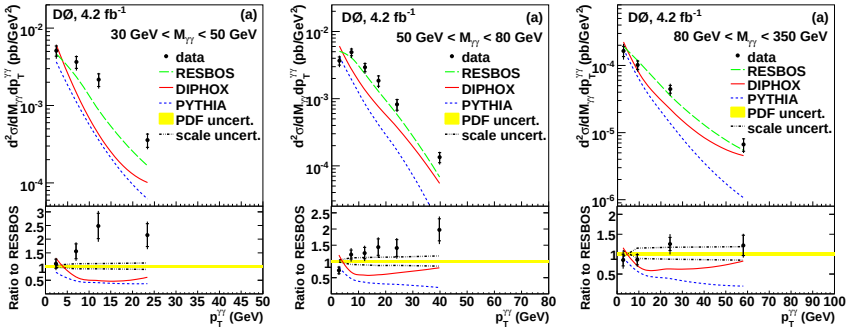

Figure 2: The measured double differential diphoton production cross sections as functions of $p_T^{\gamma\gamma}$ in three $M_{\gamma\gamma}$ intervals. The notations for points, lines and shaded regions are the same as in Fig. 1.

process will be significant. It would be interesting to see if the addition of NNLO corrections to RESBOS, as done in[8], will improve the description of the high $p_T^{\gamma\gamma}$ spectrum at low $M_{\gamma\gamma}$ region.

In summary, we present measurements of single and double differential cross sections for DPP production in $p\bar{p}$ collisions at $\sqrt{s} = 1.96\ TeV$. The analysis uses 4.2 fb^{-1} data accumulated at D0 experiment. The measured cross sections are compared to theoretical predictions from RESBOS, DIPHOX and PYTHIA, showing the necessity of including higher order corrections beyond NLO as well as the resummation to all orders of soft and collinear initial state gluons. These results allow the tuning of the theoretical predictions for this process, which is of great relevance for improving the sensitivity of searches for the Higgs boson and other new phenomena at the Tevatron and the LHC.

References

1. V.M. Abazov *et al* (D0 Collaboration), Phys. Rev. Lett. **102**, 231801 (2009)
2. T. Sjostrand *et al*, JHEP **0605**, 026(2006).
3. W.K. Tung *et al*, JHEP **0702**, 052(2007).
4. C. Balazs, E.L. Berger, S. Mrenna, and C.-P. Yuan, *Phys. Rev.* D **57**, 6934 (1998); C. Balazs, E.L. Berger, P. Nadolsky, and C.-P. Yuan, *Phys. Rev.* D **76**, 013009 (2007).
5. T. Binoth, J.P.Guillet, E.Pilon, and M. Werlen, Eur. Phys. J. C **16**, 311 (2000).
6. V.M. Abazov *et al* (D0 Collaboration), Nucl. Instrum. Methods in Phys. Res. A **565**, 463 (2006);
7. V.M. Abazov *et al* (D0 Collaboration), Phys. Rev. Lett. **102**, 231801 (2009).
8. Q.-H. Cao, C.-R. Chen, C. Schmidt, and C.-P. Yuan, arXiv:0909.2305 [hep-ph] (2009).